

Aerodynamic forces and moments on an ogive cylinder at incidence

S.C. Luo, Y.T. Ng and T.T. Lim

Department of Mechanical Engineering,
National University of Singapore, Singapore

ABSTRACT

In flows over an ogive cylinder placed at incidence, it is well documented that a side force acts on the cylinder. However, little is known about the relation between the side force (C_{Fy}) and other force and moment components. In this note, the variations of three force and three moment components, acting on the ogive cylinder, with roll angle are measured simultaneously. The model was placed at four different angles-of-attack, namely $\alpha = 30^\circ$, 45° , 50° and 60° and the results show that in addition to C_{Fy} , the variation of C_{Fz} , C_{Mx} , and C_{Mz} with the roll angle also exhibit the square wave like behaviour at $\alpha = 45^\circ$ and 50° , and with the same cross over ϕ positions, while C_{Fx} and C_{My} remain relatively constant irrespective of the roll angle. The magnitudes of C_{Fx} and C_{My} were found to increase with angle of attack and were thought to be due to the increase in normal frontal area.

1.0 INTRODUCTION

The importance of high angle of attack aerodynamics with regards to missile flight is well recognised. When the angle-of-attack (i.e. the pitch angle α) of a slender ogive body is less than 25° , symmetric trailing vortices are formed and the resultant side force acting on the body is negligible. However, at larger α , the symmetric vortical structure is replaced by a pair of asymmetric trailing vortices. The

presence of these asymmetric vortices is known to produce large side forces and yawing moments.

There are numerous investigations in the literature dedicated to the study of such flows. Lamont⁽¹⁾, Zilliac *et al*⁽²⁾, Dexter and Hunt⁽³⁾ and Luo *et al*⁽⁴⁾ showed that the variation of the side force with roll angles exhibits a square-wave-like pattern for ogive cylinders placed at intermediate angles-of-attack ($40^\circ < \alpha < 60^\circ$). This behaviour can be attributed to a sudden switch in the trailing vortex configuration as the cylinder is rolled about its axis of symmetry. Furthermore, Lamont and Hunt⁽⁵⁾ have found that the local side force exhibits a continuously decreasing but oscillatory distribution along the body/axis of the cylinder. This distribution persists for a few cycles before the local side force disappears altogether. Attempts have also been made by Owen and Johnson⁽⁶⁾, Yanta and Wardlaw⁽⁷⁾ and Wu *et al*⁽⁸⁾ to measure the circulation, vorticity and inter-vortex spatial distance of the trailing vortices, and such measurements, together with surface pressure data, have provided valuable information about the structure of the flow field and the forces acting on the cylinder body.

Given that the side force is known to be a destabilising factor in the flight of a missile, many researchers have concentrated their effort on the behaviour of the side force under different flow conditions, and provided various methods⁽⁹⁻¹³⁾ to alleviate it. However, the dynamics of a missile in flight is affected by all the three force and

three moment components. To focus solely on the side force may not give a complete picture of the aerodynamics of missile flight. Although Lamont and Hunt⁽¹⁴⁾ have presented some experimental data on the variation of the side force and yawing moment with angle of attack for an ogive cylinder, to the authors' best knowledge, no data are available for the effects of pitch and roll angle on moment and force components, apart from the side force and the yaw moment. From the available literature, there is a lack of experimental data on simultaneous force and moment measurements of flow past an inclined ogive cylinder. This apparent void in force and moment data, motivated the authors to carry out the measurements reported in this paper, which presents the results of a recent investigation conducted at the National University of Singapore on the **simultaneous** force and moment measurements (namely F_x , M_x , F_y , M_y , F_z , M_z) on a clean ogive cylinder undergoing a 360° roll, and over a range of α from 30° to 60° .

2.0 EXPERIMENTAL SET-UP

The experimental apparatus and techniques were described in detail in Luo *et al.*⁽⁴⁾ and will only be briefly described here. An open loop suction wind tunnel was used in the experiment. The test section measures 0.6m (height) \times 1.0m (width) and was operating at a free-stream velocity (U) of 15ms^{-1} . The free stream velocity was determined by using a pitot-static tube inserted into the wind tunnel test section through its ceiling and positioned right at the mid-point of the wind tunnel's cross-section, upstream of the ogive model. The pitot-static tube was removed before the commencement of any force and moment measurements to avoid introducing unnecessary flow disturbances.

The Reynolds number (Re) based on the free stream velocity and model diameter (D) of 0.035m was about 3.5×10^4 . The ogive model was inclined at an angle-of-attack (α) of 30° , 45° , 50° and 60° . These angles were selected based on the earlier studies which revealed the square-wave like behaviour of the side force coefficient (C_{F_y}) versus roll angle (ϕ) variation at $\alpha = 45^\circ$ and 50° . The total exposed length of the model in the wind tunnel was $16D$. A Nitta force balance was used to measure all the force and moment components with the resolution of $\pm 6.1 \times 10^{-3}\text{N}$ and $\pm 3.0 \times 10^{-4}\text{Nm}$ respectively, these give an error of ± 0.0482 in the force coefficients and ± 0.0043 in the moment coefficients. A computer-controlled stepper motor was used to initiate the rolling motion of the model at discrete angular increments of 7.2 degrees. At each angular position, the forces and moments were measured simultaneously over a 30-second period and all the data obtained were stored in the computer for subsequent analysis. The cylinder was then rolled to a new position, and a two-second delay was allowed for the flow to stabilise before a new set of force and moment data were acquired. Figure 1 shows a schematic of the experimental layout and the co-ordinate system used in this investigation. The important dimensions of the model are shown in the inset of the same figure. Notice that the origin of the co-ordinate system rests on the intersection point between the floor of the test section and the axis of the ogive cylinder, and all force and moment measurements were referenced to this co-ordinate system. The force coefficients were calculated by normalising the measured forces with the product of the dynamic pressure ($1/2\rho U^2$) and model cross sectional area ($\pi D^2/4$). Similarly, the measured moments were normalised with the above parameters, as well as the model length ($16D$) to yield the moment coefficients. Both the model cross sectional area and model length were kept constant throughout the experiment.

3.0 RESULTS AND DISCUSSION

The variation of force and moment coefficients with ϕ measured at $\alpha = 30^\circ$, 45° , 50° and 60° are shown in Figs 2 to 5, respectively. For

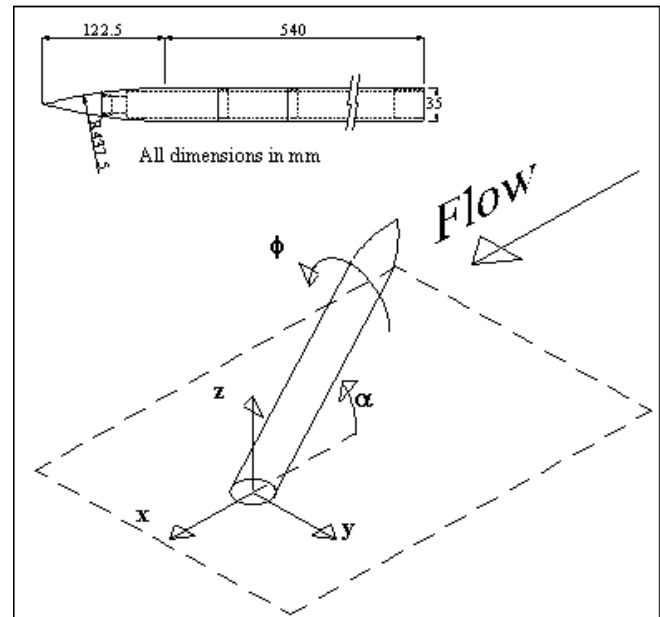


Figure 1. Experimental set-up and the Cartesian co-ordinate system for the experiment. The inset shows the important dimensions of the ogive model.

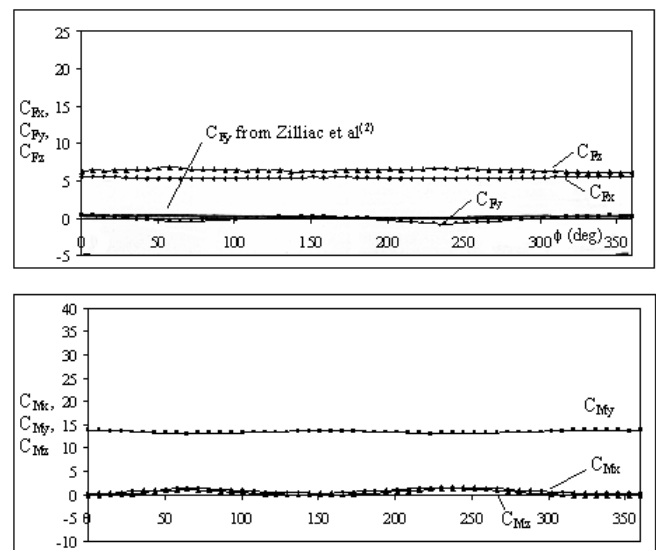


Figure 2. The variation of six force and moment coefficients with ϕ (deg) at $\alpha = 30^\circ$.

the ease of comparison among different figures, all the axes are drawn to the same scale. Comparison of the present C_{F_y} data with those of Zilliac *et al.*⁽²⁾ and Luo *et al.*⁽⁴⁾ are also shown in the figures whenever possible. As expected, the variation of side force co-efficient C_{F_y} with ϕ at $\alpha = 30^\circ$ is small and the mean is near zero (see Fig. 2), which is in good agreement with that of Zilliac *et al.*⁽²⁾. Likewise, the variation in C_{F_x} and C_{F_z} are also small, albeit at larger mean magnitudes. As for C_{M_x} , C_{M_y} , C_{M_z} , all three exhibit little variation with ϕ , but only C_{M_y} has a non-zero mean magnitude. The above observation can be attributed to the presence of a near perfectly symmetrical port-starboard time averaged vortical structure and flow field.

When the angle-of-incidence is increased to $\alpha = 45^\circ$ and 50° , the characteristic square wave like distributions of the C_{F_y} with ϕ are observed (see Figs 3 and 4), and the magnitude of C_{F_y} agrees well

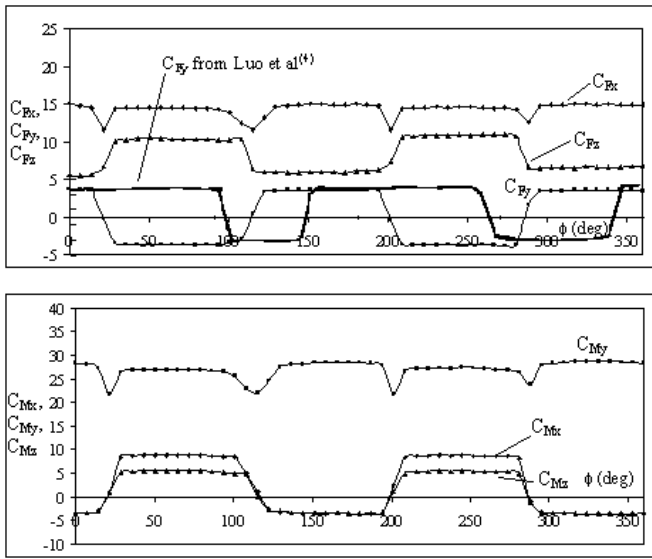


Figure 3. The variation of six force and moment coefficients with ϕ (deg) at $\alpha = 45^\circ$.

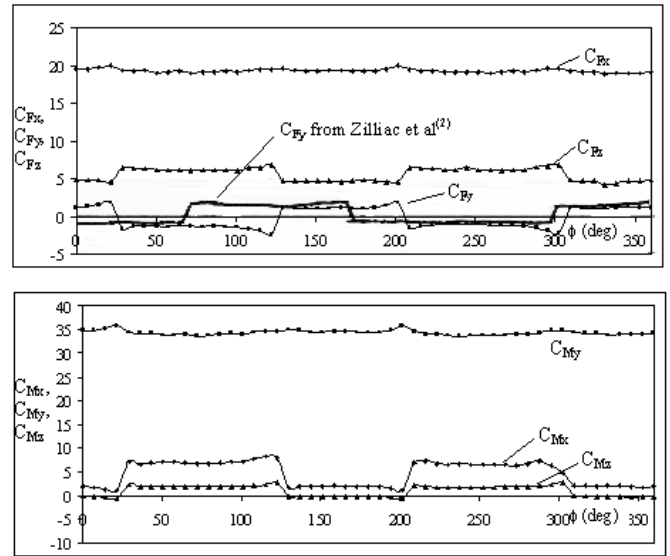


Figure 5. The variation of six force and moment coefficients with ϕ (deg) at $\alpha = 60^\circ$.

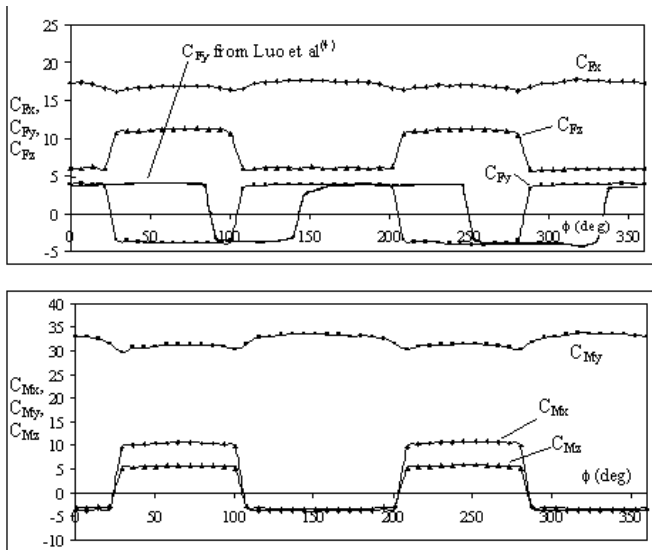


Figure 4. The variation of six force and moment coefficients with ϕ (deg) at $\alpha = 50^\circ$.

with that of Luo *et al*⁽⁴⁾, except for the cross over positions (i.e. the roll angle (ϕ) at which C_{Fy} changes sign), which are known to be sensitive to the surface geometry/conditions of the wind tunnel model. Since the surface conditions between the present and Luo *et al*⁽⁴⁾'s models cannot possibly be identical, it is of no surprise that there are differences in the cross over positions. As for C_{Fz} , C_{Mx} and C_{Mz} , similar square wave variations are found, and the corresponding cross over roll angles are akin to that of C_{Fy} , thus indicating that the switch in vortical configuration is the dominating factor. On the other hand, C_{Fx} and C_{My} for both angles of incidence deviate from the square wave pattern but their average magnitude are obviously higher than those at $\alpha = 30^\circ$.

Referring to the co-ordinate axes in Fig. 1, and based on the square wave variation of C_{Fy} with ϕ as shown in Figs 3 and 4, one would intuitively expect that a square wave variation to also appear

in C_{Mx} and C_{Mz} , but not in C_{Fx} , C_{Fz} and C_{My} . The results obtained support the above deduction except for C_{Fz} , which is contrary to our expectation. The unexpected finding suggests that the square wave response for C_{Fz} may be related to the z-distance between the body of the ogive cylinder and the trailing vortices, and warrants further investigation.

At higher α of 60° , the results presented in Fig. 5 show an attenuation in the magnitude of C_{Fy} while still maintaining a reduced square wave pattern. This finding is consistent with that of Zilliac *et al*⁽²⁾ which is also plotted in Fig. 5 for purpose of comparison. The same amplitude reduction also applies to C_{Fz} , C_{Mx} and C_{Mz} , but not C_{Fx} and C_{My} , which appear to have increased because of a larger normal frontal area that is exposed to the on coming flow as a result of the increased α .

4.0 CONCLUSION

The purpose of this paper is to establish the relation between the force and moment measurements on an ogive cylinder at high angle-of-attack. Attention was focused primary on simultaneous force and moment measurements at different roll angles. Four angles-of-attack were considered (i.e. $\alpha = 30^\circ, 45^\circ, 50^\circ$ and 60°), and the results show that in addition to C_{Fy} , the variation of C_{Fz} , C_{Mx} and C_{Mz} with the roll angle also exhibit the square wave like behaviour at $\alpha = 45^\circ$ and 50° , and with the same cross over ϕ positions, while the C_{Fx} and C_{My} remain relatively constant irrespective of the roll angle. The magnitudes of C_{Fx} and C_{My} were found to increase with angle of attack and were thought to be due to the increase in normal frontal area.

REFERENCES

- LAMONT, P.J. Pressures around an inclined ogive cylinder with laminar, transitional or turbulent separation, *AIAA J*, 1982, **20**, (11), pp 1492-1499.
- ZILLIAC, G.G., DEGANI, D. and TOBAK, M. Asymmetric vortices on a slender body of revolution, *AIAA J*, 1991, **29**, (5), pp 667-675.
- DEXTER, P.C. and HUNT, B.L. Effects of roll angle on the flow over a slender body of revolution at high angles of attack, *AIAA Paper* 81-0358, 1981.

4. LUO, S.C., LIM, T.T., LUA, K.B., CHIA, H.T., GOH, E.K.R. and HO, Q.W. Flowfield around ogive/elliptic-tip cylinder at high angle of attack, *AIAA J*, 1998, **36**, (10), pp 1778-1787.
5. LAMONT, P.J. and HUNT, B.L., Pressure and force distributions on a sharp-nosed circular cylinder at large angles of inclination to a uniform subsonic stream, *J Fluid Mechanics*, March 1976, **76**, (3), pp 519-559.
6. OWEN, F.K., and JOHNSON, D.A. Wake vortex measurement of an ogive cylinder at $\alpha = 36$ degrees, *J Aircr*, 1979, **16**, (9), pp 577-583.
7. YANTA, W.J. and WARDLAW, A.B. Jr., Flowfield about and forces on slender bodies at high angles of attack, *AIAA J*, March 1981, **19**, (3), pp 296-302.
8. WU, G., WANG, T. and TIAN, S. Investigation of vortex patterns on slender bodies at high angles of attack, *J Aircr*, 1986, **23**, (4), pp 321-325.
9. MOSKOVITZ, C.A., HALL, R.M. and DEJARNETTE, F.R. New device for controlling asymmetric flow fields on forebodies at large alpha, *J Aircr*, 1991, **28**, (7), pp 456-462.
10. ASGHAR, A., STAHL, W.H. and MAHMOOD, M. Suppression of vortex asymmetry and side force on a circular cone, *AIAA J*, 1992, **32**, (10), pp 2117-2120.
11. RAO, D.M. Side force alleviation on the slender, pointed forebodies at high angles of attack, *J Aircr*, 1979, **16**, (11), pp 763-768.
12. LUA, K.B., LIM, T.T., LUO, S.C. and GOH, E.K.R. Helical-groove and circular-trip effects on side force, *J Aircr*, 2000, **37**, (5), pp 906-915.
13. LEE, A.S., LUO, S.C., LIM, T.T., LUA, K.B. and GOH, E.K.R. Side force on an ogive cylinder: Effects of control devices, *AIAA J*, 2000, **38**, (3), pp 385-388.
14. LAMONT, P.J. and HUNT, B.L. Prediction of aerodynamic out of plane forces on ogive nosed circular cylinder, *J Spacecraft Rockets*, 1977, **14**, (1), pp 38-44.